Supplemental material:

Lateral size of graphene oxide determines differential cellular uptake and cell death pathways in Kupffer cells, LSECs, and hepatocytes

Jiulong Li [a,b], *Xiang Wang* [a,b], *Kuo-Ching Mei* [a,b], *Chong Hyun Chang* [a,b], *Jinhong Jiang* [a,b], *Xiangsheng Liu* [a,b], *Qi Liu* [a,b], *Linda M. Guiney* [c], *Mark C. Hersam* [c], *Yu-Pei Liao* [a,b], *Huan Meng* [a,b,d], *Tian Xia* [a,b,d,*]

[a] Center of Environmental Implications of Nanotechnology (UC CEIN), University of California, Los Angeles, CA 90095, USA

[b] California NanoSystems Institute, University of California, Los Angeles, CA 90095, USA

[d] Division of NanoMedicine, Department of Medicine, University of California, Los Angeles, CA 90095, USA

[c] Departments of Materials Science and Engineering, Chemistry, and Medicine, Northwestern University, Evanston, IL 60208, USA

*Corresponding Author: Tian Xia, M.D./Ph.D.,

Department of Medicine, Division of NanoMedicine, UCLA School of Medicine, 52-175 CHS, 10833 Le Conte Ave, Los Angeles, CA 90095-1680.

E-mail: txia@ucla.edu

22

23

24

25

Figures

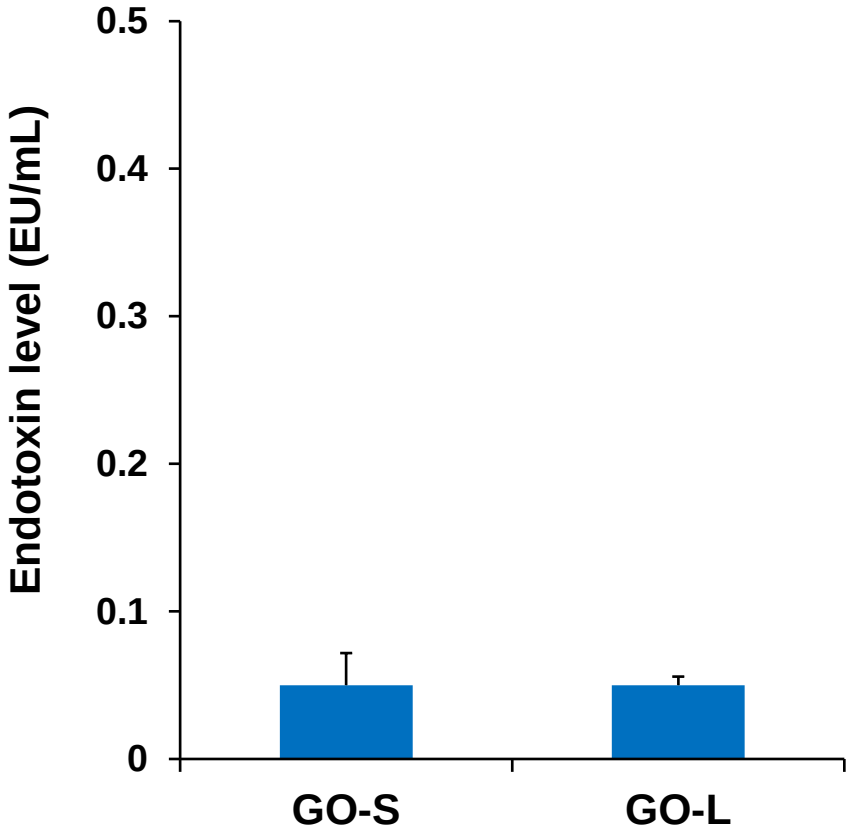

Fig. S1. The endotoxin level of GOs suspended at 50 μg/mL in DI water was determined using a Limulus Amebocyte Lysate assay kit (Lonza, Walkersville, MD). The endotoxin limit (for medical devices) recommended by the FDA is 0.5 EU/mL.

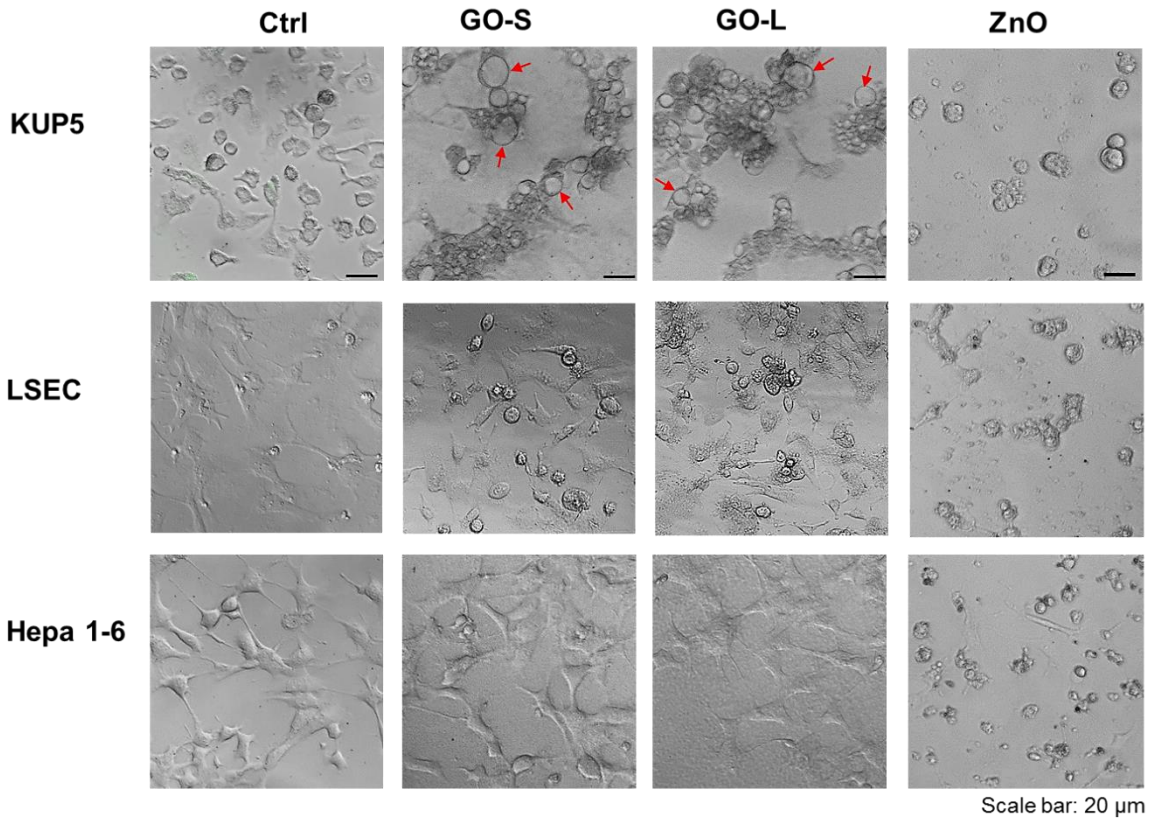

Fig. S2. Optical microscope images to compare the KUP5, LSEC, and Hepa 1-6 cell morphological changes by GO. The cells were exposed to 12.5 μg/mL GO for 16 h at 37 °C and 5% CO_2 in a 12-well plate, respectively. The morphology of the cell was monitored using a Zeiss Optical Microscope **(**Carl Zeiss Microscopy LLC, White Plains, NY, USA**)**. Red arrows indicate significant morphological changes by GO sheets in cells. The scale bar in the image is 20 μm.

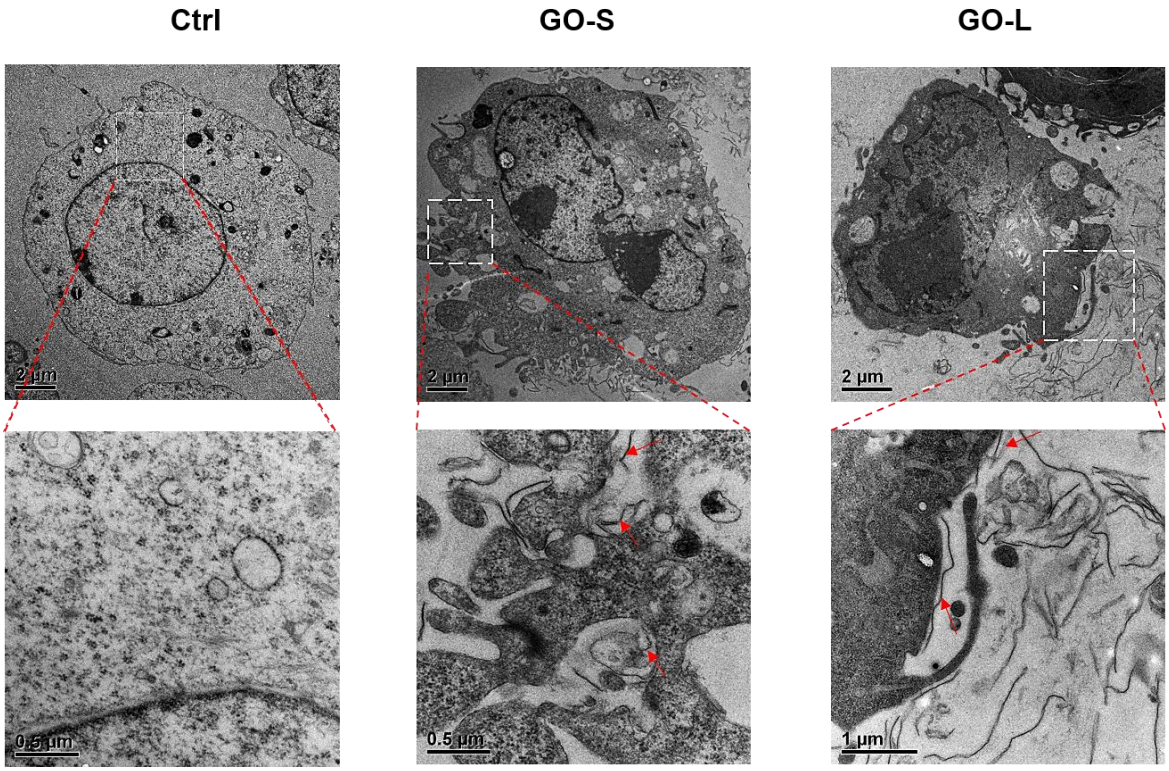

Fig. S3. Visualizing the interactions of GO with LSECs by TEM. After exposure to 50 μg/mL of GO for 16 h, the cells were washed, fixed, and stained for TEM viewing under a JEOL 1200-EX TEM with an accelerating voltage of 80K eV. Red arrows indicate GO sheets within the cytosol or on the plasma membrane. TEM images for untreated cells were also shown. Scale bar in the upper row is 2 μm; Scale bar in the lower row is 0.5 or 1 μm.

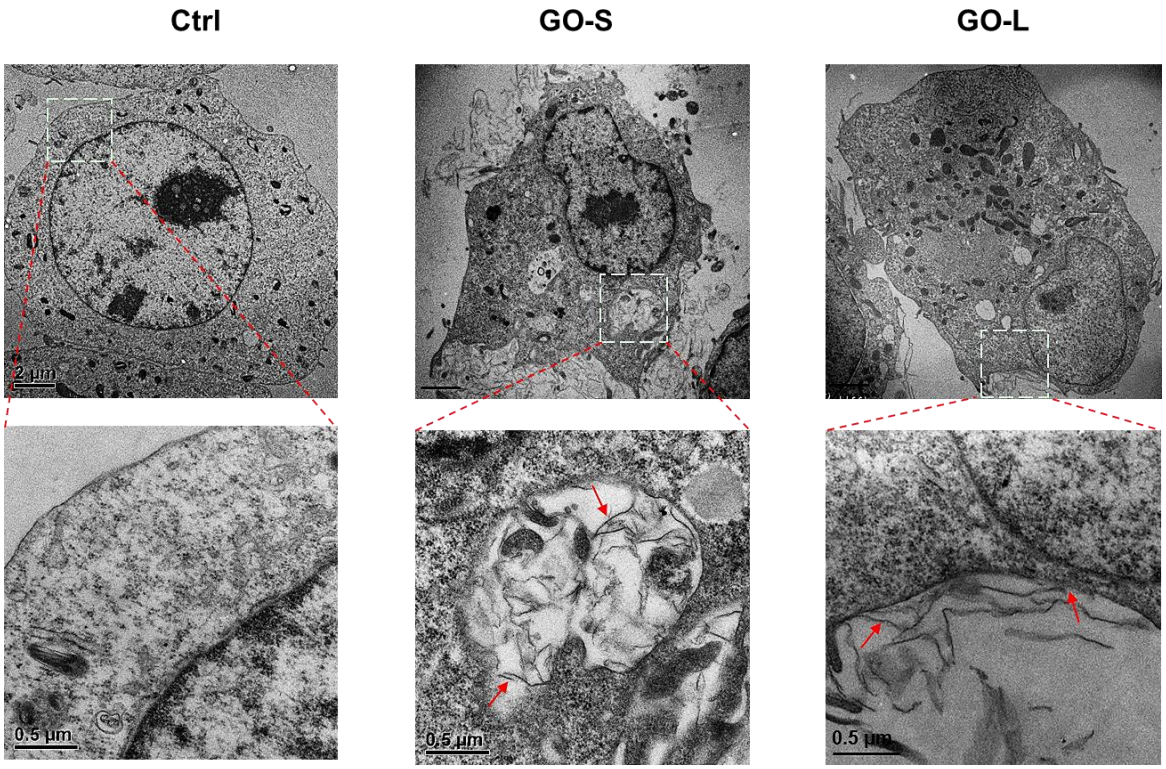

Fig.S4. Visualizing the localization of GO in Hepa 1-6 cells by TEM. After exposure to 50 μg/mL of GO for 16 h, the cells were washed, fixed, and stained for TEM viewing. Red arrows indicate GO sheets within the cytosol or on the plasma membrane. TEM images for untreated cells were also shown. Scale bar in the upper row is 2 μm; Scale bar in the lower row is 0.5 μm.

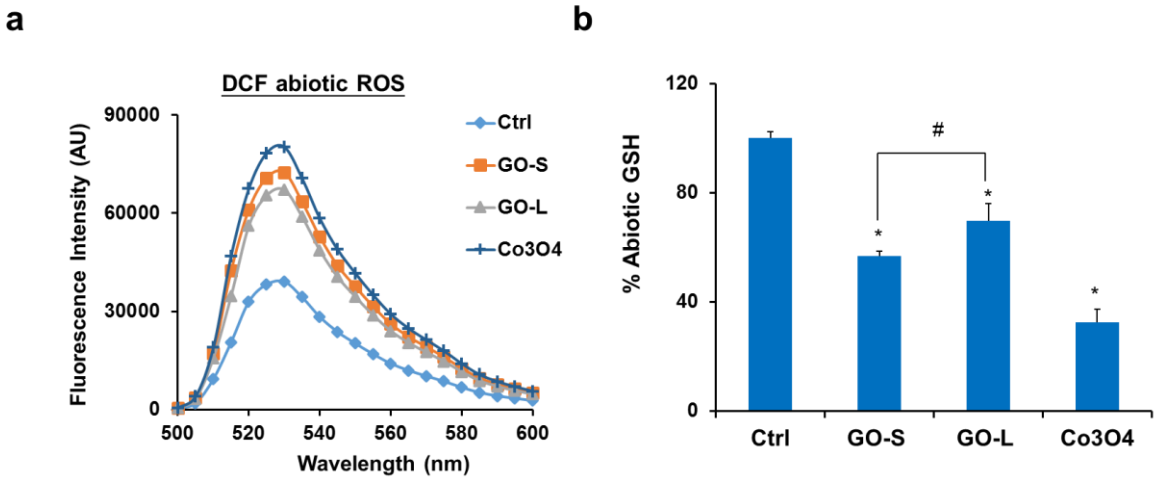

Fig. S5. Determination of intrinsic oxidative stress of GOs. (a) The abiotic ROS generation by 50 μg/mL of GO was determined by H_2DCFDA fluorescence. DCF fluorescence emission spectra in the range of 500–600 nm were collected with an excitation wavelength of 490 nm. The treatment of Co_3O_4 was set as a positive control. (b) Assessment of the abiotic GSH content was performed by adding 10 μL of GOs at 50 μg/mL to a 96-well plate together with 90 μL of GSH-Glo agent for 30 min. The luminescence was detected by a SpectraMax M5e microplate reader. The treatment of Co_3O_4 was set as a positive control. Asterisk (*) means $P < 0.05$, compared to the control, and #, $P < 0.05$, indicates significance between GO-S and GO-L treatments.

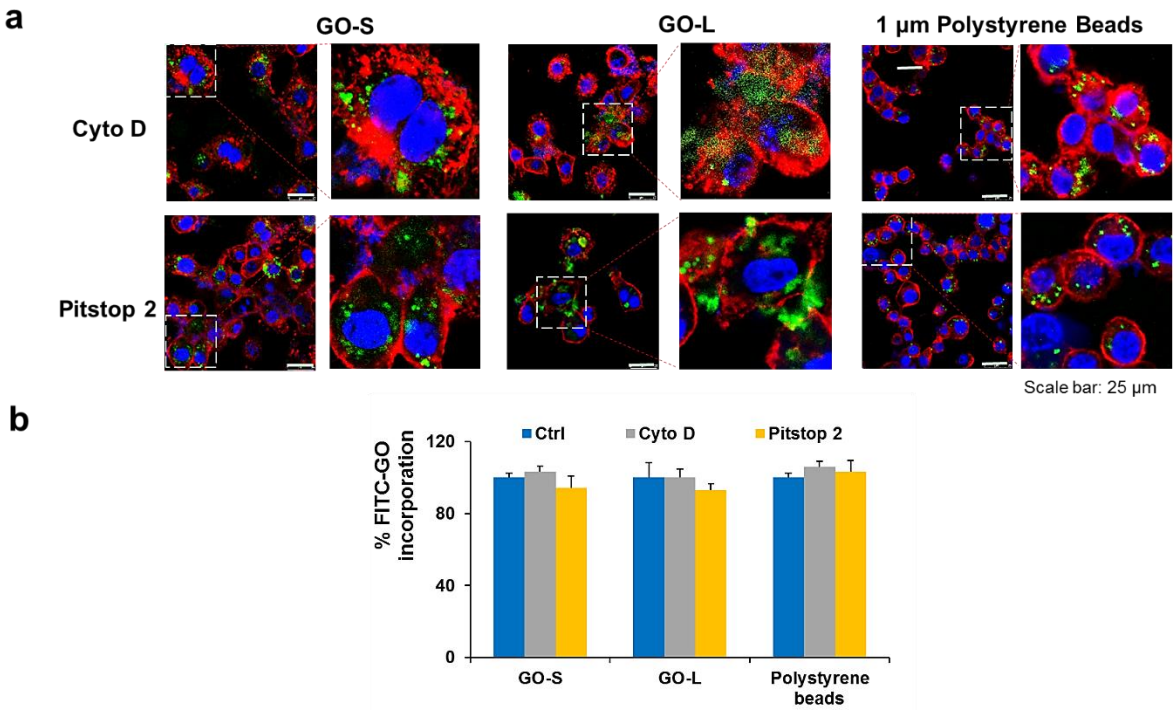

Fig. S6. Effects of cellular uptake inhibitor on FITC-GOs incorporation in KUP5 cells. (a) Confocal images to determine the cellular localization of FITC-GO in KUP5 cells under the cellular uptake inhibitor treatments. Before exposure to GO, KUP5 cells were treated with 5 μg/mL of cytochalasin D for 1 h and 20 μM of pitstop 2 for 0.5 h, respectively. After staining with Hoechst 33342 dye and Alexa Fluor 594-labeled WGA antibody, the cells were visualized under a Leica Confocal SP8-SMD confocal microscope. The scale bar in the left panel image is 25 μm. (b) Quantification for the effects of cellular uptake inhibitor on FITC-GOs incorporation in KUP5 cells by a fluorescence microplate reader.

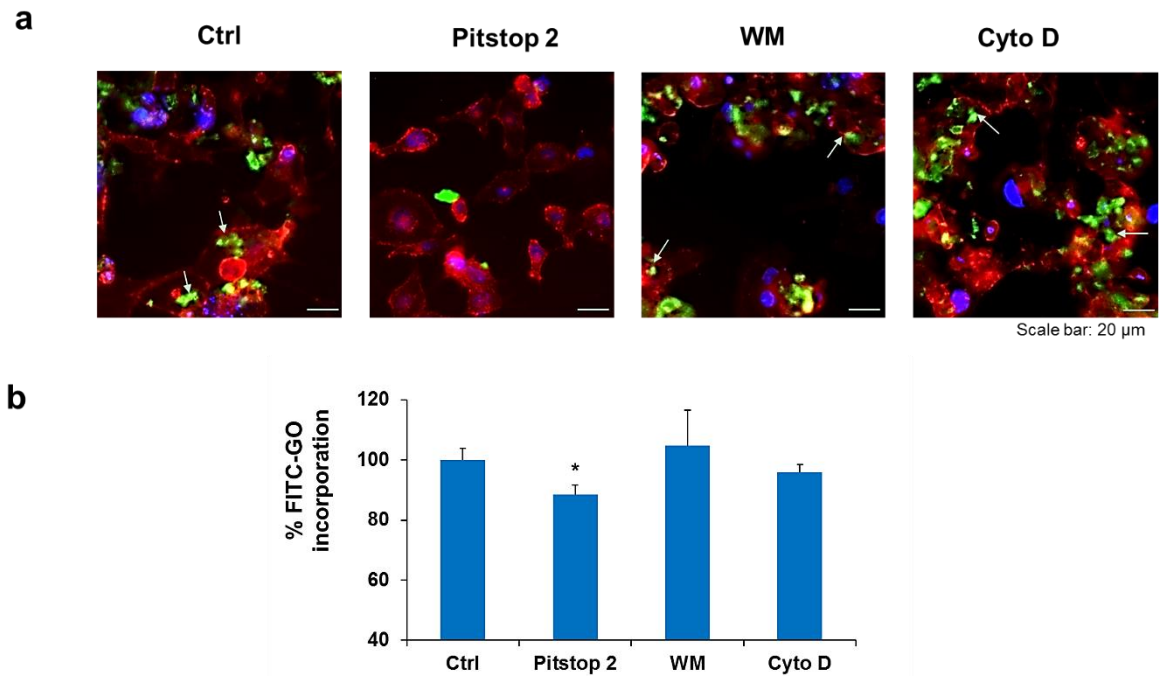

Fig. S7. Effects of cellular uptake inhibitor on FITC-GOs incorporation in LSECs. (a) Representative fluorescence images to determine the cellular localization of FITC-GO in LSECs under the cellular uptake inhibitor treatments. Before exposure to GO, cells were treated with 20 μM of pitstop 2 for 0.5 h, 1 μM of wortmannin for 0.5 h, and 5 μg/mL of cytochalasin D for 1 h, respectively. White arrows indicated the uptake GO inside cells. The scale bar is 20 μm. (b) Quantification for the effects of cellular uptake inhibitor on FITC-GOs incorporation in LSECs by a microplate reader. *, $P < 0.05$, indicates significance compared to the control.

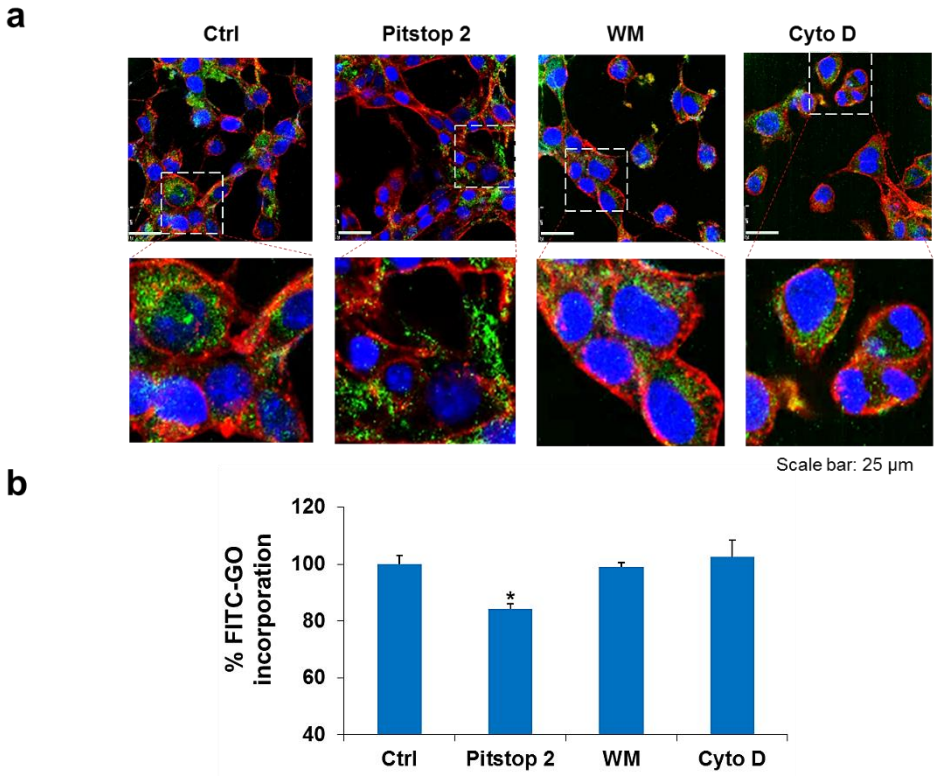

Fig. S8. Effects of cellular uptake inhibitor on FITC-GOs incorporation in Hepa 1-6 cells. (a) Representative confocal images to determine the cellular localization of FITC-GO in Hepa 1-6 cells under the cellular uptake inhibitor treatments. Before exposure to GO, Hepa 1-6 cells were treated with 20 μM of pitstop 2 for 0.5 h, 1 μM of wortmannin for 0.5 h, and 5 μg/mL of cytochalasin D for 1 h, respectively. The scale bar in the left panel image is 25 μm. (b) Quantification for the effects of cellular uptake inhibitor on FITC-GOs incorporation in Hepa 1-6 cells by a microplate reader. *, $P < 0.05$, indicates significance compared to the control.

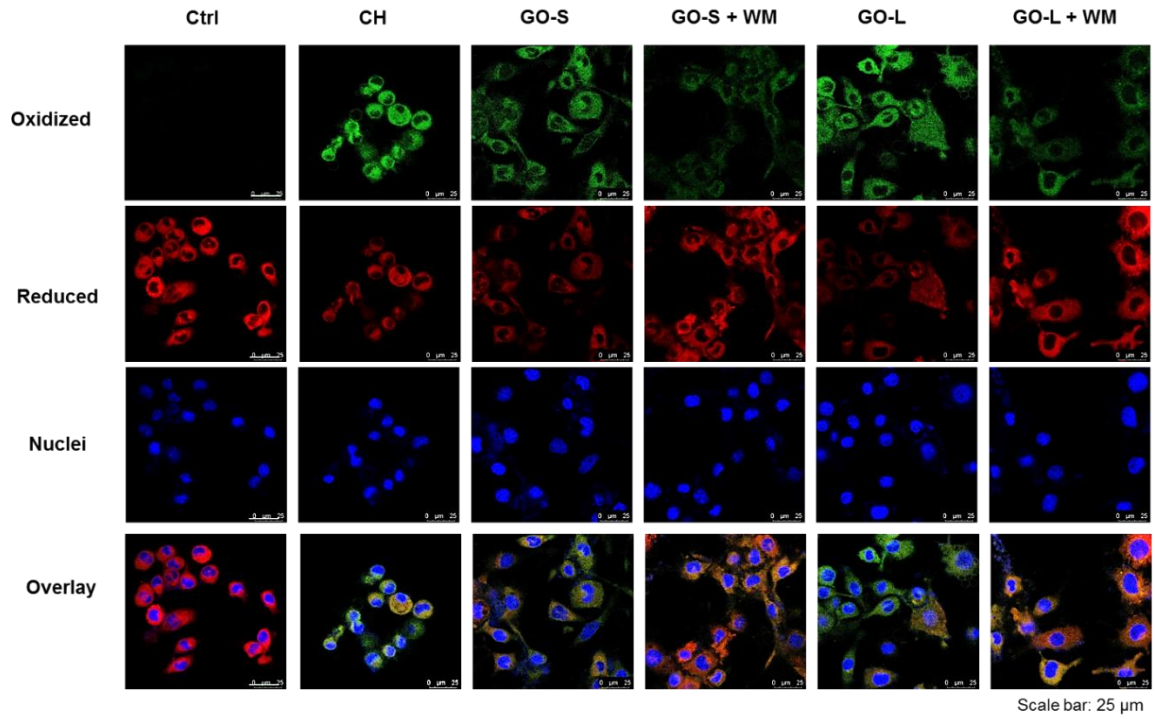

Fig. S9. Assessment of the plasma membrane lipid peroxidation production by GO in KUP5 cells pretreated with WM. Confocal images to demonstrate the reduction of lipid peroxidation production in KUP5 cells. The images were acquired to visualize the reduced (red) and oxidized (green) fluorescent dye at excitation/emission wavelengths of 581/591 nm and 488/510 nm. The scale bar is 25 μm.

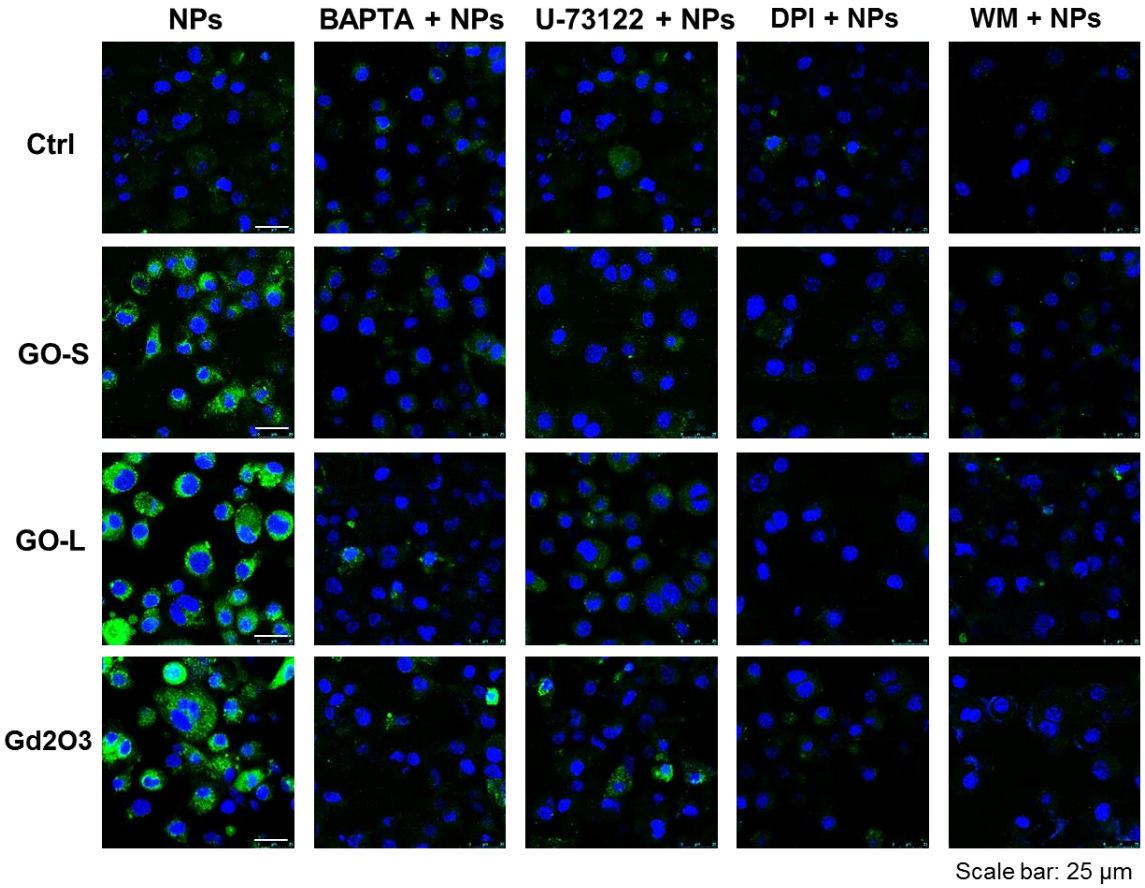

Fig. S10. Intercellular calcium accumulation assessed by confocal microscopy. KUP5 cells were pretreated with or without inhibitors (BAPTA as calcium chelator and U-73122 used as PLC inhibitor, DPI used as NADPH oxidase, WM used as phagocytosis inhibitor) before treatment of 12.5 μg/mL of GO or Gd_2O_3 for 16 h. Cells were stained with 5 μM of Fluo-4 AM ester (green) for 60 min and Hoechst 33342 (blue) for 15 min. The scale bar is 25 μm.

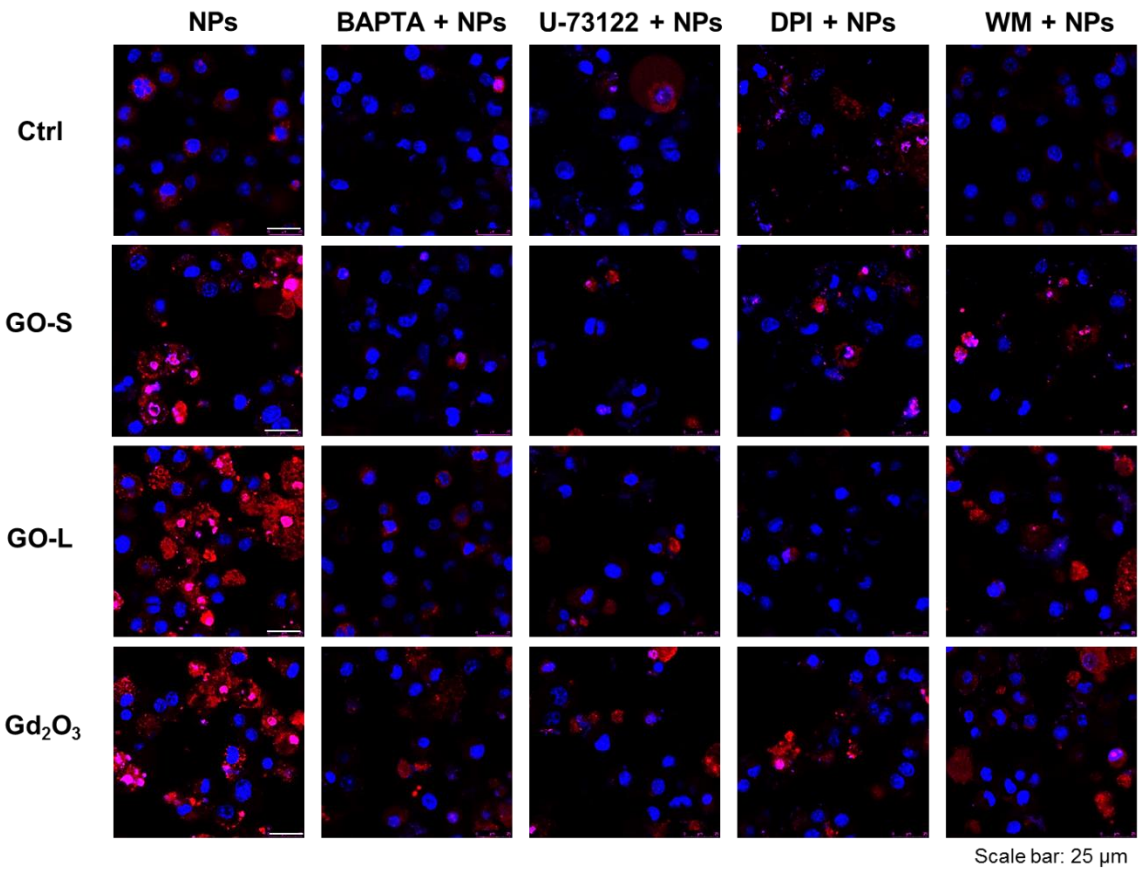

Fig. S11. Cellular mitochondrial ROS generation in KUP5 cells post-exposed to GO. KUP5 cells were pretreated with or without inhibitors BAPTA, U-73122, DPI, and WM before exposure to 12.5 μg/mL of GO or Gd_2O_3 (positive control) for 16 h. Cells were stained with 5 μM of red MitoSOX and Hoechst 33342 for 15 min, respectively. The scale bar is 25 μm.

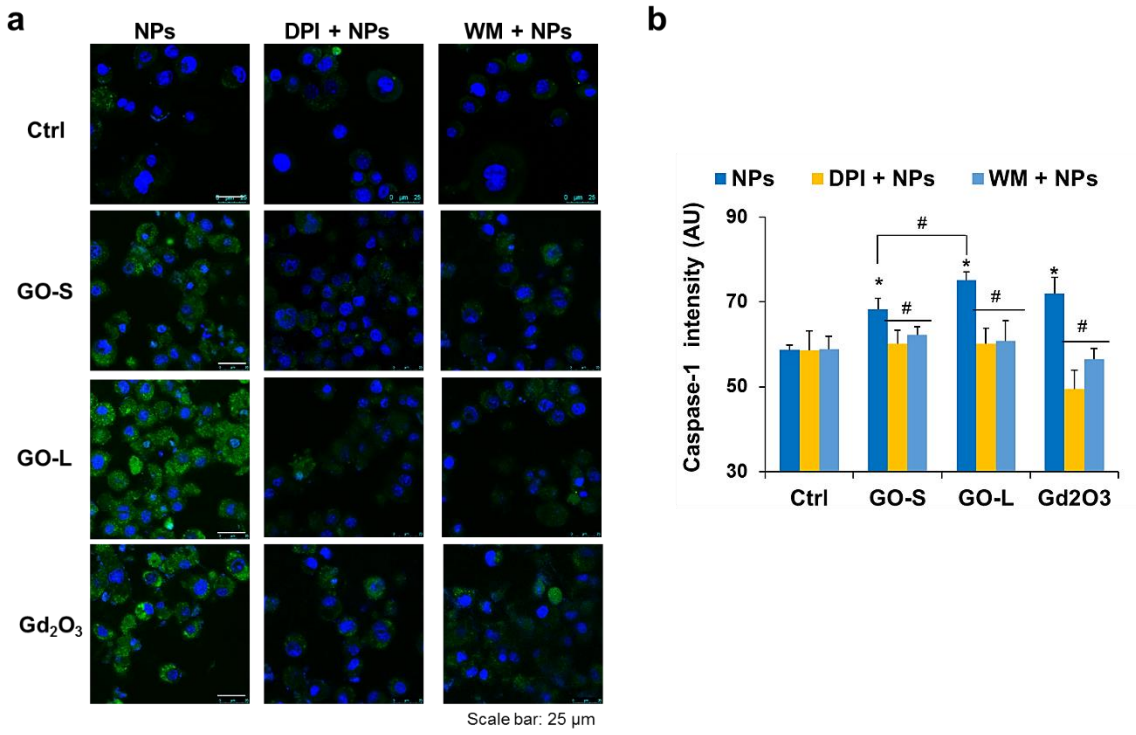

Fig. S12. Effect of various inhibitors on caspase-1 activation in GO-treated KUP5 cells. (a) The LPS-primed KUP5 cells were incubated with various inhibitors (DPI used as NADPH oxidase inhibitor and WM used as phagocytosis inhibitor) were exposed to 12.5 μg/mL GO or Gd_2O_3 (positive control) for 16 h. Cells washed with PBS were stained with FAM-FLICA caspase substrate (green) for 1 h, stained with Hoechst 33342 for 15 min, and imaged using Leica Confocal SP8-SMD microscope. The scale bar is 25 μm. (b) Quantification for caspase 1 activation in KUP5 cells under GO treatments with inhibitors. The fluorescence intensity was monitored at excitation/emission wavelengths of 492/520 nm. *, $P < 0.05$, indicates significance compared with the control; #, $P < 0.05$, indicates significance compared to NP treatment alone.

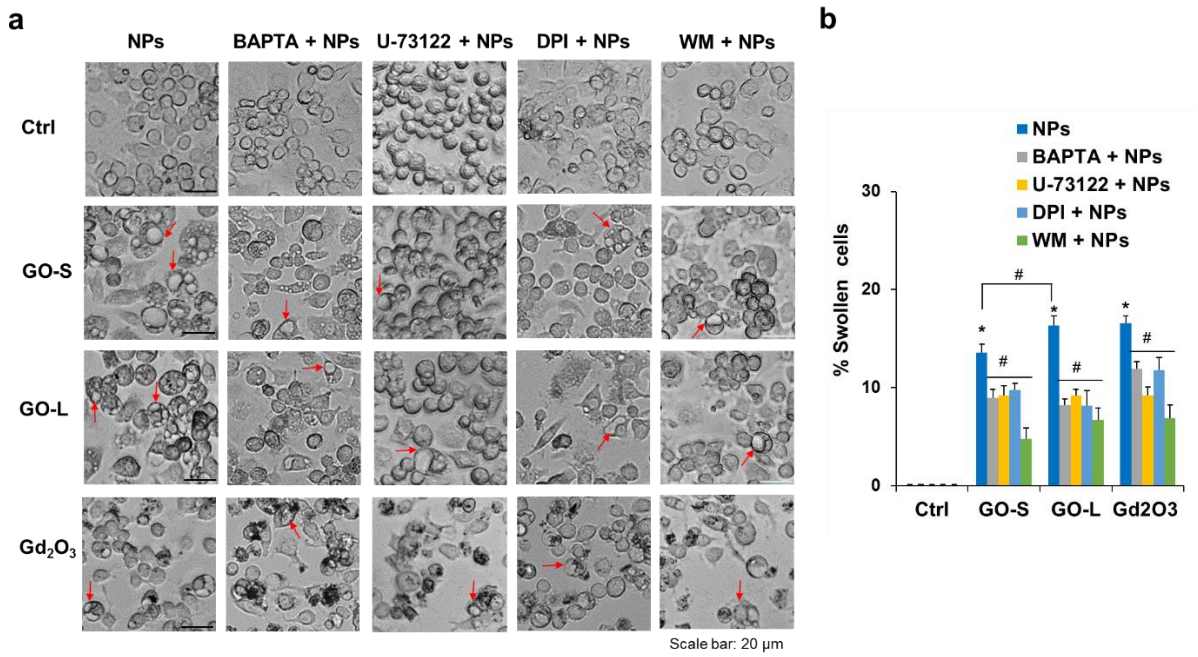

Fig. S13. Effect of various inhibitors on pyroptosis in KUP5 cells. (a) Optical microscope images to compare the GO-treated KUP5 cell morphological changes by various inhibitors (BAPTA used as calcium chelator, and U-73122 used as PLC inhibitor, DPI, and WM). Red arrows indicate the swollen cells. The scale bar is 20 μm. (b) The percentage of swollen cells was calculated based on the cells expressing at least two giant blebs in KUP5 cells treated with various inhibitors before 12.5 μg/mL of GO or Gd_2O_3 exposure for 16 h. *, $P < 0.05$, indicates significance compared with the control; #, $P < 0.05$, indicates significance compared to NP treatment alone.

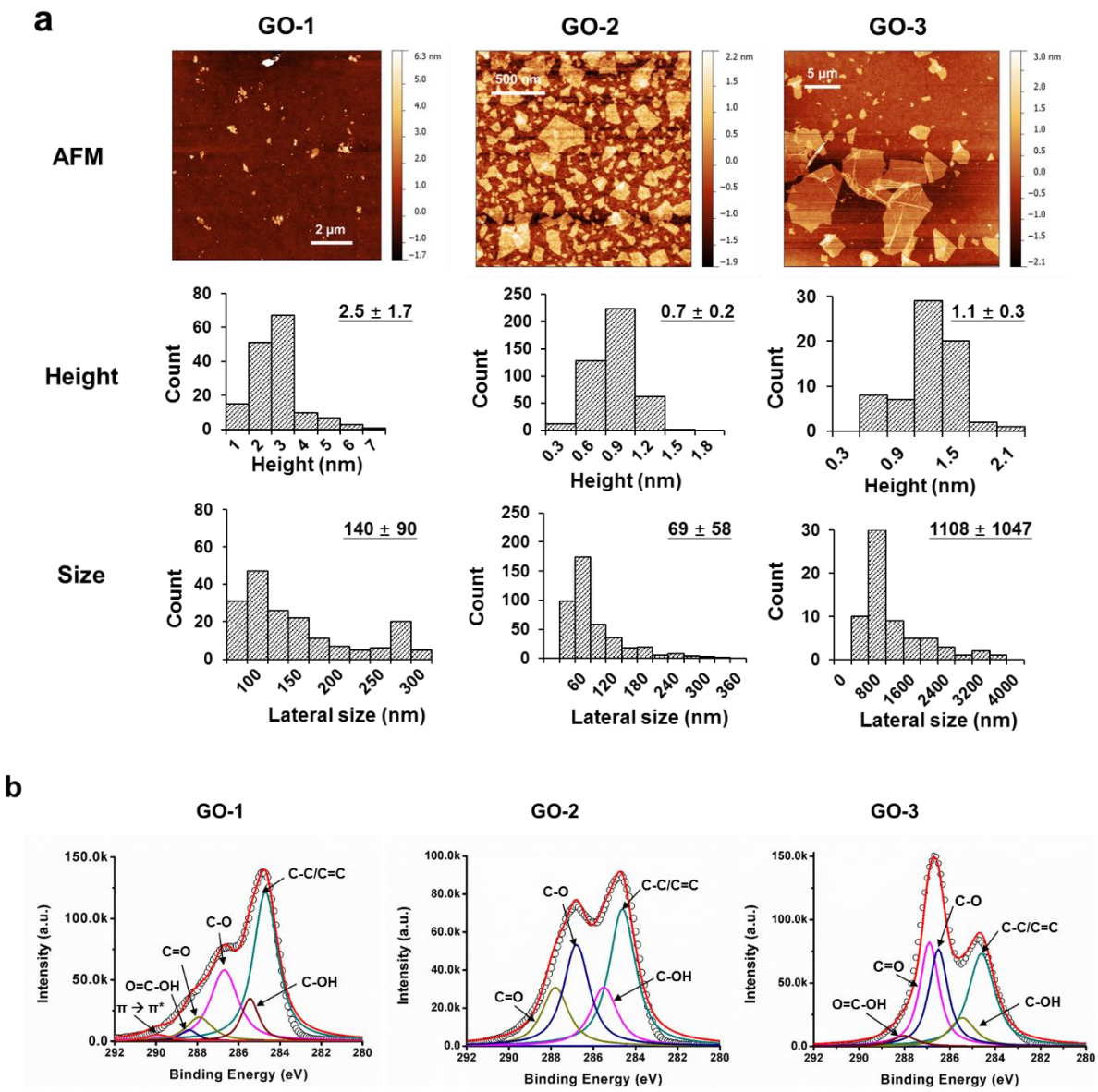

Fig. S14. Characterization for differential physicochemical properties among GO-1, GO-2, and GO-3 samples. (a) Characterization of GO-1, GO-2, and GO-3 through AFM analysis. The panels in the top row show the histograms of GO height distributions. The average height of GO-1 is 2.5 ± 1.7 nm, the average height of GO-2 is 0.7 ± 0.2 nm, and the average height of GO-3 is 1.1 ± 0.3 nm. The panels in the bottom row show the histograms of GO lateral size distributions. The average lateral size of GO-1, GO-2, and GO-3 is 140 ± 90, 69 ± 58, and 1108 ± 1047 nm, respectively. (b) C 1s XPS spectra of GO-1, GO-2, and GO-3.

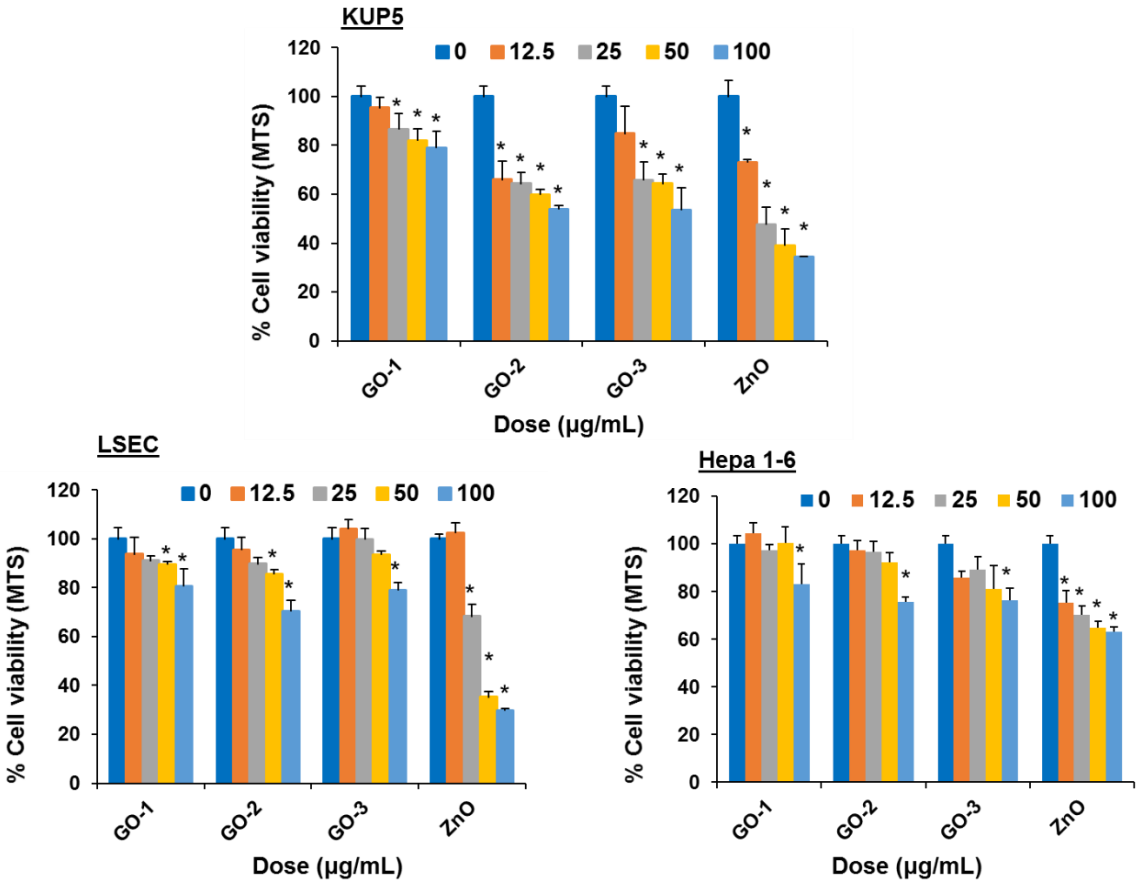

Fig. S15. Cell viability of KUP5, LSEC, and Hepa 1-6 cells on GOs exposure for 24 h at a dose range of 0−100 μg/mL determined by MTS assay. The viability of untreated control cells was set to 100%. Asterisk (*) means $P < 0.05$, compared to the control. KUP5 cells were more sensitive to the cytotoxic effects of GOs than LSECs and Hepa 1−6 cells.

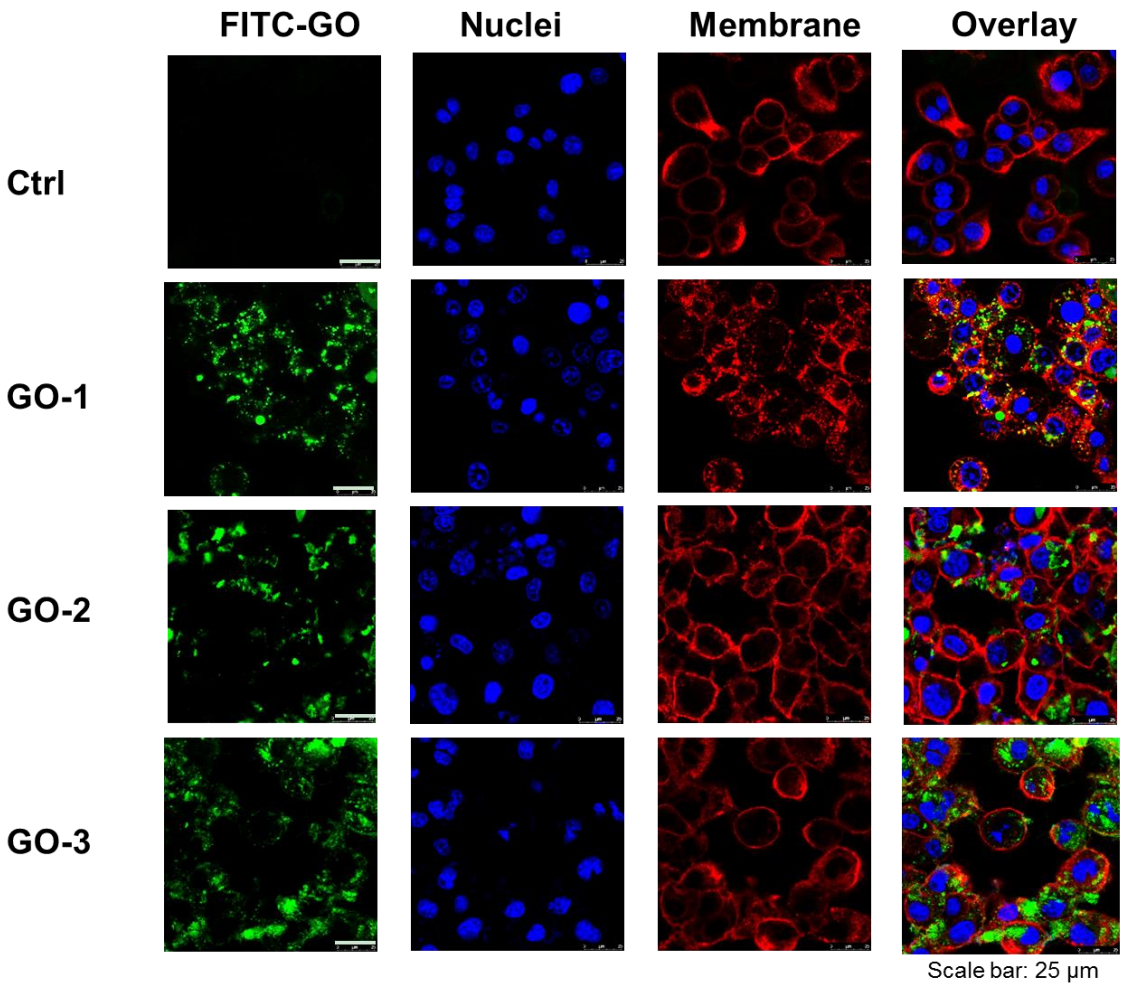

Fig. S16. Determination of cellular localization of GO-1, GO-2, and GO-3 in KUP5 cells using confocal imaging. KUP5 cells were incubated with 12.5 μg/mL of FITC-labeled GOs (green) for 16 h, followed by staining with Hoechst 33342 dye (blue) and Alexa Fluor 594-labeled WGA antibody (red). The scale bar is 25 μm.

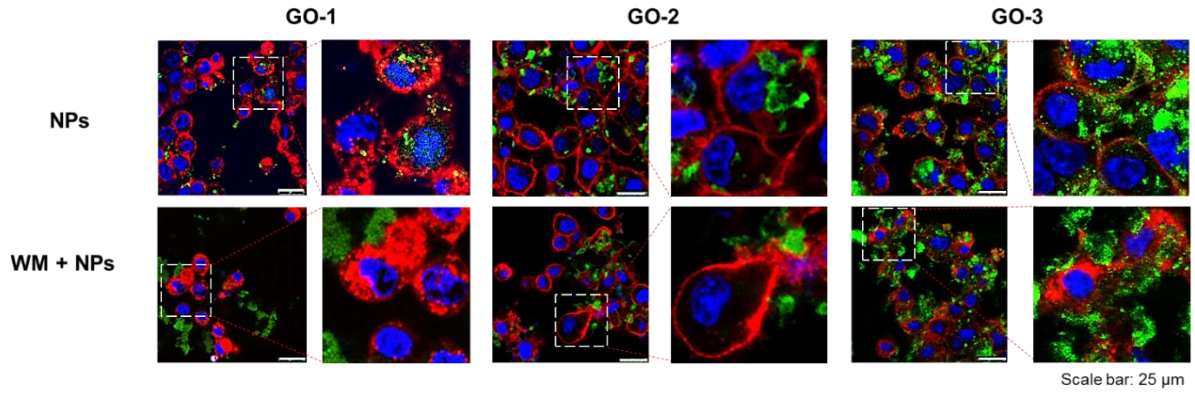

Fig. S17. Representative confocal images to determine the phagocytosis of GO-1, GO-2, and GO-3 by KUP5 cells. Before exposure to FITC-GOs, KUP5 cells were pretreated with 1 μM WM for 0.5 h. After staining with Hoechst 33342 dye and Alexa Fluor 594-labeled WGA antibody, the cells were visualized under a confocal microscope. The scale bar in the left panel is 25 μm.

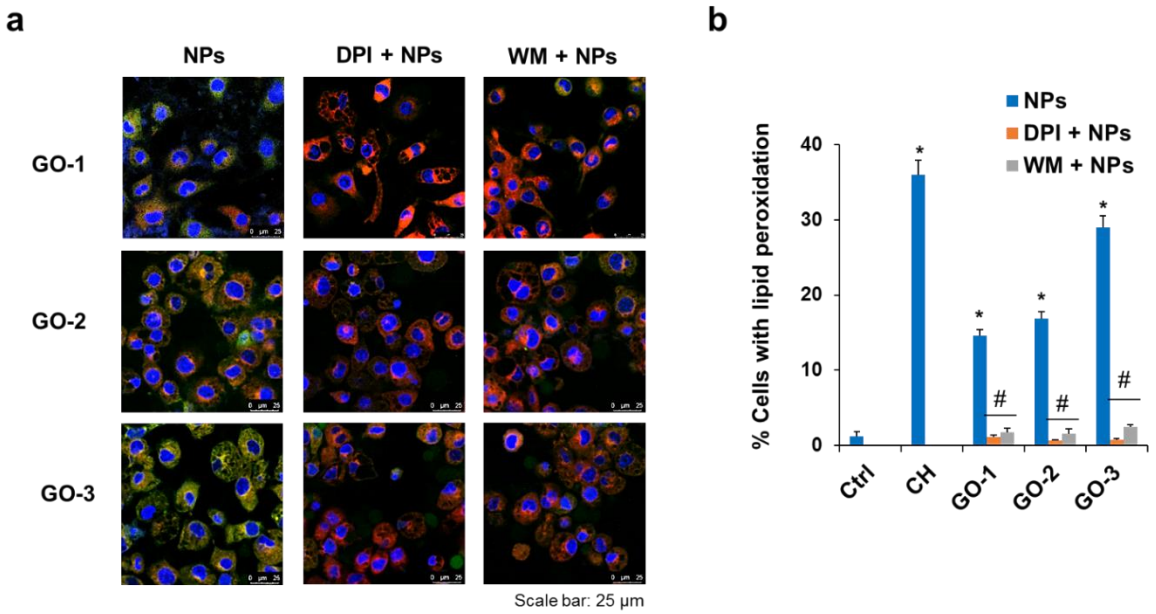

Fig. S18. Assessment of the plasma membrane lipid peroxidation production by GO-1, GO-2, and GO-3. (a) Confocal images to demonstrate the reduction of lipid peroxidation production in KUP5 cells pretreated with an NADPH oxidase inhibitor DPI and a phagocytosis inhibitor WM, respectively. The images were acquired to visualize the reduced (red) and oxidized (green) fluorescent dye at excitation/emission wavelengths of 581/591 nm and 488/510 nm. The scale bar is 25 μm. (b) Quantification for the percentage of cells with lipid peroxidation induced by GO-1, GO-2, and GO-3 by flow cytometry. *, $P < 0.05$, indicates significance compared with the control; #, $P < 0.05$, indicates significance compared to GO treatment alone.

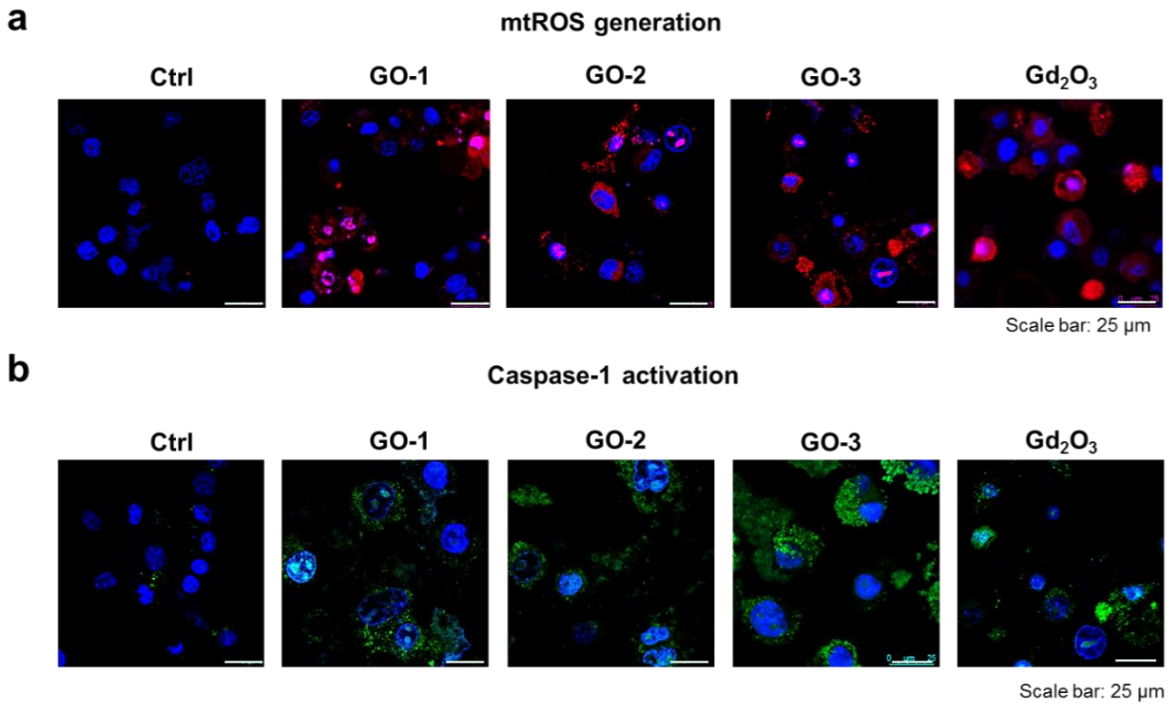

Fig. S19. Determination of the mtROS generation and caspase-1 activation in KUP5 cells treated with GO-1, GO-2, and GO-3. (a) MtROS generation was assessed by confocal microscopy. KUP5 cells exposed to 12.5 μg/mL of GOs or Gd_2O_3 (positive control) for 16 h were stained with 5 μM of red MitoSOX and Hoechst 33342 for 15 min, respectively. (b) Assessment of caspase-1 activation in GO-treated KUP5 cells. The LPS-primed KUP5 cells were washed with PBS, stained with FAM-FLICA caspase substrate (green) for 1 h and Hoechst 33342 for 15 min, and imaged using Leica Confocal SP8-SMD microscope. The scale bar is 25 μm.

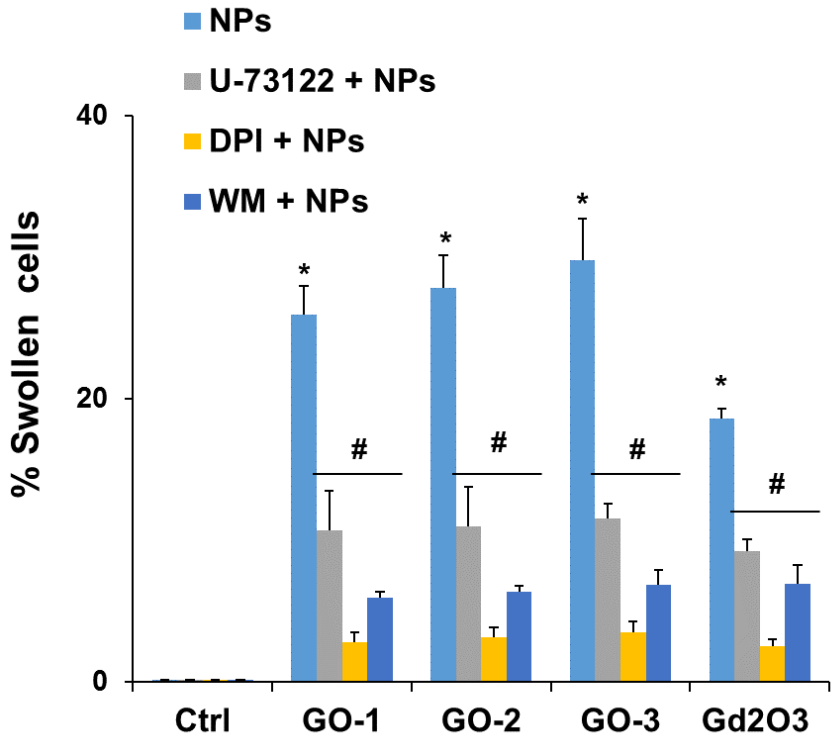

Fig. S20. Effect of various inhibitors on cells swelling by GO-1, GO-2, and GO-3. The percentage of swollen cells was calculated based on the cells expressing at least two giant blebs in KUP5 cells pretreated with various inhibitors, including U-73122 used as a PLC inhibitor, DPI used as an NADPH oxidase inhibitor, and WM used as an inhibitor on cellular uptake of GO. *, $P < 0.05$, indicates significance compared with the control; #, $P < 0.05$, indicates significance between GO treatments without and with inhibitors.

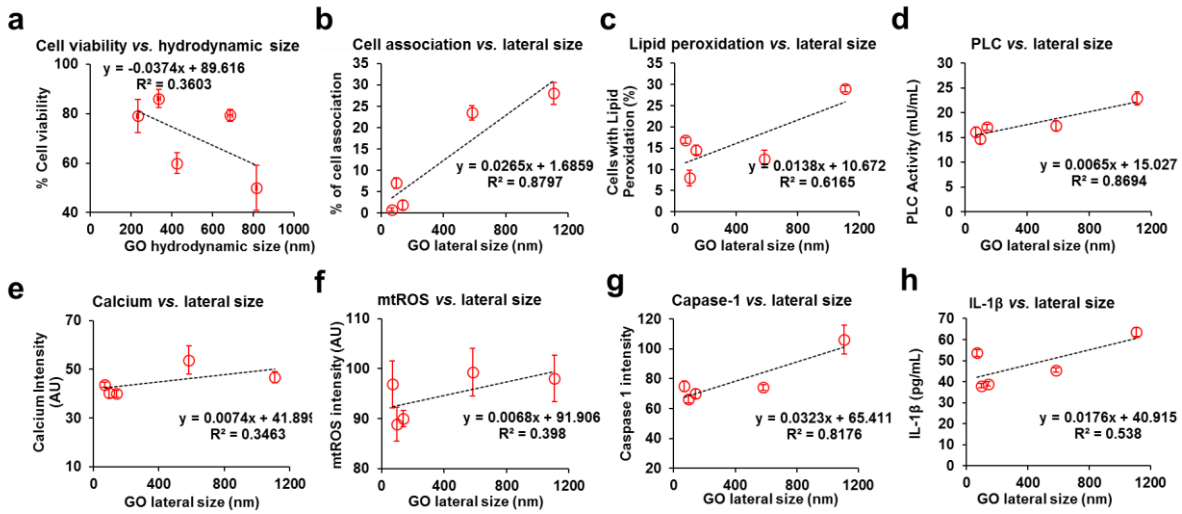

Fig. S21. The correlation plots of the GO in KUP5 cells. (a) The plotting of the GO hydrodynamic size showed correlation coefficients with cell viability. (b-h) Plotting of the GO lateral size (AFM) showed excellent correlation coefficients with cell association (b), lipid peroxidation (c), PLC activation (d), calcium flux (e), mtROS generation (f), caspase-1 activation (g), as well as IL-1β release (h).

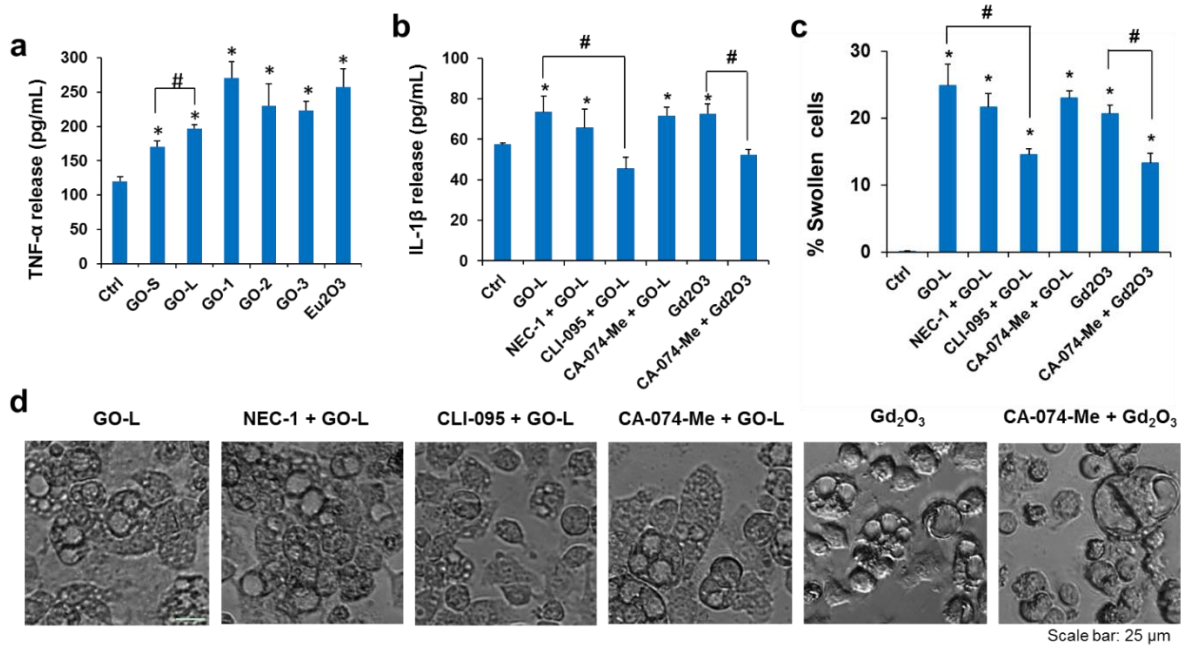

Fig. S22. TNF-α production, IL-1β release, and cell swelling in GO-treated KUP5. LPS-primed (1 μg/mL, 4 h) KUP5 cells were pretreated with 30 nM of necroptosis inhibitor NEC-1 (necrostatin-1) overnight, 1 μg/mL of CLI-095 (TLR4 inhibitor) overnight, and 30 μM of the cathepsin B inhibitor CA-074-Me for 6 h, respectively, before GO exposure. Supernatants were collected to measure TNF-α (a) and IL-1β (b) release by ELISA, respectively. The percentage of swollen cells (c) was calculated based on the cells expressing at least two giant blebs in KUP5 cells (d) pretreated with various inhibitors. The scale bar is 20 μm. *, $P < 0.05$, indicates significance compared with the control; #, $P < 0.05$, indicates significance between GO treatments

Table

Tab S1. Hydrodynamic size, polydispersity index, and zeta potential of GO in different media.

Media	Sample	Hydrodynamic size (nm)	Polydispersity index (PDI)	Z-potential (mV)
DI H2O	GO-1	148.0 ± 1.1	0.2	-40.7 ± 2.0
	GO-2	260.3 ± 0.6	0.3	-59.86 ± 1.3
	GO-3	417.8 ± 14.3	0.3	-51.57 ± 2.4
DMEM (KUP5)	GO-1	233.8 ± 4.2	0.2	-7.5 ± 1.8
	GO-2	426.4 ± 0.5	0.3	-10.2 ± 0.6
	GO-3	815.5 ± 2.8	0.3	-11.4 ± 1.9
Prigrow medium (LSEC)	GO-1	172.6 ± 5.2	0.2	-11.1 ± 1.7
	GO-2	327.1 ± 4.1	0.3	-11.4 ± 3.6
	GO-3	529.4 ± 14.2	0.3	-12.3 ± 2.4
DMEM (Hepa 1-6)	GO-1	217.6 ± 1.9	0.2	-10.9 ± 1.9
	GO-2	345.3 ± 15.1	0.3	-9.7 ± 2.5
	GO-3	816.8 ± 29.3	0.3	-7.5 ± 0.6